


Skin penetration and UV-damage prevention by nanoberrries

Paula Bucci MSc¹ | María Jimena Prieto PhD¹ | Laura Milla PhD² |
María Natalia Calienni MSc¹ | Luis Martinez MSc¹ | Viviana Rivarola PhD² |
Silvia Alonso PhD¹ | Jorge Montanari PhD¹ 

¹Laboratory of Biomembranes - GBEyB (IMBICE, CCT-La Plata, CONICET), Departamento de Ciencia y Tecnología, National University of Quilmes, Bernal, Argentina

²Department of Molecular Biology, National University of Río Cuarto, Río Cuarto, Córdoba, Argentina

Correspondence

Jorge Montanari, Lab of Biomembranes, National University of Quilmes, Bernal, Buenos Aires, Argentina.
Email: jmontanari@unq.edu.ar

Summary

Background: Ethanolic extract from blueberry (*Vaccinium myrtillus*) is rich in anthocyanins and thus exhibits antioxidant activity. On the other hand, ultradeformable liposomes are capable of penetrating to the impermeable barrier of skin. Nanoberrries are ultradeformable liposomes carrying blueberry extract.

Objectives: In this study, their capacity to penetrate the *stratum corneum* and photodamage prevention were tested, with the aim of developing a topical formulation for skin protection from environmental damage.

Methods: Nanoberrries were prepared by lipid film resuspension with ethanolic extract from blueberry, followed by sonication and incorporation to a gel. Size, zeta potential, deformability, rheology, and viscoelasticity were determined. Toxicity was assessed in vivo in zebrafish model, while in vitro cytotoxicity assay was performed on HaCaT and HEK-293T cell lines. Skin penetration was evaluated with the Saarbrücken penetration model followed by tape stripping, cryosection, or optical sectioning. UV-damage protection and photoprotection were determined by ad hoc methods with UVA, UVB, and UVC radiation on HaCaT cells. Wound assay was performed on HaCaT cells.

Results: Nanoberrries of about 100 nm, with differential elastic properties, did penetrate the *stratum corneum*, with low toxicity. When HaCaT cells were exposed to UV radiation in the presence of nanoberrries, their viability was maintained.

Conclusions: Nanoberrries could be effective to protect the skin from sun photodamage.

KEYWORDS

blueberry, nanocosmetics, ultradeformable liposomes, UV damage, zebrafish

1 | INTRODUCTION

Polyphenols are a wide group of compounds, of special interest as cosmetic and therapeutic active principles for the skin, due to their antioxidant properties. The antioxidant activity is related to their hydroxyl and aromatic groups.¹ Blueberry (*Vaccinium myrtillus*) contains great amount of these compounds,² mainly anthocyanins, that are highly soluble in water and, besides their antioxidant properties, their anti-inflammatory activity has been also described, among

others.³ The total amount of anthocyanins in blueberry is around 6 g per kg of fruit.² Natural antioxidants are specially relevant in comparison with synthetic compounds, because of the potential carcinogenicity of the latter.⁴ Nevertheless, oral consumption of blueberry is not enough to achieve good biodistribution of antioxidants because of very low absorption at intestinal level (less than 1%)⁵ and the rapid metabolization after passing through the intestine epithelium. On the other hand, the intermolecular hydrogen bonds reduce their chances of diffusion through biological membranes.⁶

Free radicals, generated by the action of UV radiation, oxide compounds in the cells causing damage and activating cellular mechanisms that attack molecules such as collagen, which brings structure and support to the skin.⁷ Thus, long-life exposure to UV radiation becomes the main environmental factor that causes skin aging.⁸ Besides, UV radiation is also a risk factor in the development of different types of skin cancer.⁹ Thus, both aesthetic and health factors are involved in this problematic, which, despite prevention campaigns, are not sufficiently known by the many different risk groups.¹⁰ Because of this, we propose the idea of a topical nanoformulation for the direct supply of blueberry antioxidants, with the aim of protecting the skin *in situ* from the attack of reactive species generated by UV rays. Recent research has shown that ethanolic extracts rich in phenolic compounds can effectively protect skin-derived cells from UV damage.¹¹

In this context, the nanoberries (NB) were developed,¹² based on ultradeformable liposomes, made of soy phosphatidylcholine and sodium cholate. In these kinds of liposomes, the sodium cholate makes the membrane deformable at room temperature, by drastically lowering its elastic modulus in comparison with conventional liposomes,¹³ thus allowing them to penetrate through the *stratum corneum* (SC) impelling their content to the viable epidermis while conventional liposomes cannot go through the impermeable barrier of SC.¹⁴ This differential feature makes the ultradeformable liposomes useful for many applications in nanomedicine¹⁵ and potentially for nanocosmetics.¹⁶ Biophysical characterization of NB showed low cytotoxicity, high antioxidant activity, and good stability parameters.¹²

In this work, we studied the ability of NB to transport their antioxidant compounds through the SC *ex vivo*, *in vivo* toxicity, and *in vitro* protective effect against different kinds of UV radiation.

2 | MATERIALS AND METHODS

2.1 | Materials

Soybean phosphatidylcholine (SPC), sodium cholate (NaChol), Sephadex G-50, Folin-Ciocalteu reagent, gallic acid, dimethyl-thiazolyltetrazolium bromide (MTT), 1,2-dipalmitoyl-sn-glycerol-3-phosphoethanolamine-N-lissamine rhodamine B sulphonyl (Rhodamine-PE), and fluorescein isothiocyanate (FITC) were purchased from Sigma-Aldrich (St. Louis, MO). Other reagents were of analytical grade, from Anedra (Tigre, Argentina). Blueberries were donated by The Berry Store (San Pedro, Argentina).

2.2 | Blueberry extract (BE) obtention

An ethanolic extract from blueberry (*Vaccinium myrtillus*, "Millenia" variety) rich in antioxidants was obtained by the process described by Montanari et al. (2012).¹² Briefly, 25 g of fruit (harvested in December 2015 at latitude 33°45'S, longitude 59°45'W, elevation 36 m) was ground, and then, 150 mL of ethanol (96%) was added at 0.1% HCl, followed by bath sonication (75 minutes at 25°C, 40 kHz)

and then filtering under vacuum through Whatman No. 1 filter. Ethanol and water from the fruit were eliminated under rotary evaporation (30°C, 200 rpm) at low pressure, up to constant weight. The process rendered about 0.1 g of extract per gram of fresh fruit. Additionally, as a control, the antioxidant activity of the extract was determined as in that previous work, obtaining similar values: The concentration that effectively reduced a 50% (IC₅₀) of a free radical (1,1-diphenyl-2-picrylhydrazyl, DPPH, from Sigma-Aldrich [St. Louis, MO]) was 0.75 mg of extract per mL, whereas the total antioxidant activity at that concentration (determined by the linoleic-beta carotene method) was higher than 90%, with similar values after incorporation to liposomal formulations.

Total polyphenolic compounds were determined by the method of the Folin-Ciocalteu reagent using gallic acid as standard.¹⁷ Monomeric anthocyanins were determined by the spectrophotometric pH differential method¹⁸ using cyanidin-3-glucoside as absorbance standard.

2.3 | Preparation of Nanoberries

Nanoberries (NB), that is, BE-loaded ultradeformable liposomes, were prepared according to Montanari¹² based on the work of Cevc for ultradeformable liposome obtention.¹³ Briefly, a mix of SPC and NaChol (6:1 w/w) in CHCl₃:CH₃OH (1:1 v/v) was flash-evaporated at 40°C in a round-bottom flask until all total evaporation of solvents. The thin lipid film on the flask was then rehydrated in a 6.13 mg/mL solution of BE in 10 mM Tris-HCl buffer at 0.9% NaCl, pH 7.4, up to a final concentration of 40 mg SPC/mL. The suspension was submitted to sonication (3 cycles, 30 seconds each, with 30-seconds resting intervals, at 10 000W) to reduce size and lamellarity.

In addition to this formulation, nonultradeformable nanoberries (NUNB) were prepared without NaChol, multilamellar nanoberries (MNB) were prepared without the sonication step, empty ultradeformable liposomes (EUL) were prepared without the addition of the BE to the resuspension buffer, and double-labeled fluorescent nanoberries in their ultradeformable (FNB) or nonultradeformable (FNUNB) form were prepared by adding Rh-PE to the lipid mix (1:1000, Rh-PE:SPC, mol:mol) and FITC to the resuspension buffer. For these fluorophore-labeled formulations, fluorescent nonincorporated compounds were separated by gel filtration chromatography in a Sephadex G-50 column by the method of Fry.¹⁹ Finally, some aliquots of NB suspension were incorporated to a Carbopol gel (NB-C) based on the method of Al-Suwayeh,²⁰ in a ratio of 100 μ L of NB to 10 mg of Carbopol 940 per mL of distilled water.

3 | CHARACTERIZATION

Particle size and ζ -potential of NB were determined with a Nanozetasizer (Malvern Instruments, Malvern, Worcestershire, UK). Structure was studied by scanning electronic microscopy (SEM) after submitting samples to vacuum dry in the presence or absence of cryoprotectant (20% sucrose).²¹

The rheology for NB-C in comparison with a Carbopol gel without NB (C) was studied by flux resistance determination at 4°C and 37°C, by a screening of shear rates from 0 to 400 s⁻¹. For viscoelasticity studies, at first, a stress sweep step was performed to determine the linear viscoelastic region, from which a shear stress (τ) value was chosen. Then, the shear storage modulus (G') and shear loss modulus (G'') were determined by a frequency sweep step (ω) at the fix τ . All the rheology and viscoelasticity studies were realized with an AR-G2 rheometer provided with Advantage Software (TA Instruments Ltd, Dallas, TX), with a cone-plate geometry of 40 mm in diameter and cone angle of 2°. The gap used in the distance plate-cone was 55 μ m.

3.1 | In vivo nanotoxicity in zebrafish model

3.1.1 | Animals

Sexually mature adult zebrafish (*Danio rerio*), 8-12 months old, were maintained at 28.0 \pm 1.0°C in aquaria (aerated, pH 7.0-8.0) under a 14-h/10-h light/dark cycle. Embryos were produced by natural mating, as described by Prieto et al²². Briefly, fish were crossed by placing them (3:2 female-to- male ratio) in plastic mesh traps. Only fertilized eggs in optimal conditions were selected for the study after observation with a stereomicroscope (Leica Zoom 2000, Wetzlar, Germany). Three days postfertilization (dpf), embryos hatch, and from that moment on (over 3 dpf), we refer to zebrafish as larvae. Embryos and larvae used in this work were transferred to conditioned E3 medium (NaCl 5 mM, KCl 0.17 mM, CaCl₂ 0.33 mM, MgSO₄ 0.33 mM) with 50 ppb methylene blue to inhibit fungal growth, and reared at 28.5°C on a 14-h/10-h light/dark cycle.

3.1.2 | Ethic use of animals

The animal procedures described here were performed strictly in accordance with the NIH guidelines for animal care and maintenance. All protocols were approved by the Institutional Animal Care Committee, National University of Quilmes (Resolution CE-UNQ 2/2014) (Buenos Aires, Argentina).

3.1.3 | Measurement of locomotor activity

For this study, 48 hours postfecundation (hpf), in each well of a 96-well plate containing E3 medium, nonhatched zebrafish embryos were placed and incubated for 48 h more, at 28°C. At 4 dpf, the medium was replaced by 250 μ L of solutions of NB, BE, EUL, or E3 (as control), in serial dilutions until final concentrations of 0.325 μ g/mL of BE (or the corresponding concentration of lipids for EUL). Three replicates were used for each dilution in every triplicate of this assay. Swimming activity was recorded during 15 minutes at 4, 5, 6, and 7 dpf, after inoculation with the formulation tested, at room temperature with a multichannel ADC system (WMicrotracker, Designplus SRL, Argentina) that detects the refraction of infrared beams through the zebrafish bodies.²³ Variations over 3% of the

signal received (an empirical threshold previously determined) were considered as activity events. Swimming activity was calculated summing up the number of activity events for 15 minutes. Data were reported as average activity events for each infrared beam pair \pm SEM. Finally, the lethal dose 50 (LD₅₀) was determined for each treatment at 7 dpf by counting dead larvae with a trinocular magnifying glass.

3.2 | Skin penetration experiments

3.2.1 | Sample preparation and incubation

To assess ex vivo human skin penetration of NB, the Saarbrücken penetration model (SPM)²⁴ was used. Explants from a Caucasian female patient (healthy, with no medical history of skin diseases) taken after an abdominal plastic surgery were cleaned with buffer, and the fatty tissue was removed with a scalpel. Skin disks of 25 mm in diameter were punched out and transferred into the SPM device, with a filter paper soaked in Tris buffer at the bottom of the Teflon block, with the *stratum corneum* (SC) facing up.

BE solution (6.13 mg/mL in Tris buffer), NB, NUNB, or NB-C was applied to skin disks without occlusion, in all cases at 70 μ g of BE/cm², and incubated during 1 h at 35°C.¹⁴ Similar amounts in lipids were applied in the same way for FNB and FNUNB.

3.2.2 | Tape stripping and optical segmentation

Some skin specimens were segmented by mounting the skin disks on a polystyrene block using pins to stretch the tissue, then covering them with a Teflon mask with a 15-mm window at the center, and successively stripping the skin with 20 pieces of adhesive tape charged with a 2-kg weight during 10 s before remotion.¹⁴

The tapes from FNB incubation were collected individually, while for all the other formulations, tapes were collected in three groups: tapes 1-3 corresponding to shallow SC (sSC), tapes 4-10 to medium SC (mSC), and tapes 11-20 to deep SC (dSC). BE from all the formulations was extracted from the tapes with 2 mL of ethanol:water (1:1 v/v) under constant agitation (190 rpm) for 1 h at 37°C. BE was quantified by measuring absorbance at 546 nm with a spectrophotometer Jasco V-550 (Jasco, Easton, MD) with Spectrum Manager software. Rh-PE and FITC were extracted the same way, and their emissions (587 nm and 517 nm, respectively) were quantified upon excitation at 570 nm and 495 nm, respectively, with a FluoroMate FS-2 fluorometer (Scinco, Seoul, Korea) with SimpleRead software.

The remains of the skin below the SC—the viable epidermis and the dermis—were ground, followed by extraction and BE or fluorescence determination as stated for the tapes. All the experiments were carried out in quintuplicate, and blanks from tape strips or full skin thickness from nonincubated samples were subtracted.

Other skin samples, after incubation with FNB, were optically scanned at 3- μ m intervals along the z-axis (20 images from 0 to 60 μ m of depth at 20X) with an Olympus FV3000 (Olympus, Center Valley, PA) confocal laser scanning microscope (CLSM) equipped

with an Ar laser (488 nm) and a He-Ne laser (543 nm) for FITC and Rh-PE excitation, respectively. Images were analyzed with ImageJ software, and the fluorescence of each dye was quantified.

3.2.3 | Skin cryosectioning

Other skin disks were incubated with FNB. Following, they were embedded in OCT after incubation and rapidly frozen at -80°C . Slices of 20 μm thickness (perpendicular to the skin) were obtained with a cryomicrotome Leica CM 1850 (Leica, Wetzlar, Germany) at -20°C . Slices were then fixed in formaldehyde (5 minutes at 10%, and then washed three times with PBS) and later observed by CLSM. Some slices from the same specimens were also stained by hematoxylin-eosin to confirm the absence of histological alterations in the tissues (data not shown).

3.3 | Protection from photodamage in cell culture

3.3.1 | Cells

To study whether NB or BE could protect the lowering of cell viability after exposure to UV radiation, assays were performed in HaCaT—a cell line derived from human keratinocytes—and in HEK-293T cells (a very different cell line, of kidney origin). For all the experiments, cells were seeded in 96-well plates initially at 5×10^3 cells per well, and then grown for 24 h before incubation and/or irradiation. Cells were cultured in RPMI or D-MEM (Gibco, Life Technologies, Carlsbad, CA) for HaCaT and D-MEM for HEK-293T, supplemented with 10% fetal calf serum (FCS), 1% antibiotic/antimycotic (PAA, Pasching, Austria) (penicillin, streptomycin sulfate and amphotericin B), and 2 mM glutamine, at 37°C in 5% CO_2 and 95% humidity. Eight wells were used for each condition of incubation or irradiation, and the experiments were repeated three times.

3.3.2 | Cytotoxicity assays

Cells were incubated with different concentrations of NB or BE. Cytotoxicity was determined by the MTT technique²⁵ to find an atoxic range of work. Empty ultradeformable liposomes (i.e., NB without BE) were used as control.¹²

3.3.3 | Photodamage determination

For the determination of photodamage, ad hoc irradiation systems were prepared: Plates were seeded with HaCaT or HEK-293T cells, leaving two empty columns between the seeded ones. Seeded rows were covered with black tape and thick aluminum foil. The plates were placed into boxes holding tubes emitting UVA (380 nm–400 nm) or UVB (310 nm–320 nm) in the upper part of their interior, and, for UVC radiation (254 nm), plates were placed into a Stratallinker UV 1800 Crosslinker (Stratagene, La Jolla, CA). Tape and aluminum foil were progressively retired to expose columns to different energy doses,

leaving a nonirradiated control. Thirty minutes or twenty-four hours after exposure, MTT assay was performed to determine the lowering of viability as a function of the radiation dose. The experiment on HaCaT cells was performed with UVA, UVB, and UVC, while for HEK-293T, it was only carried out with UVC.

3.3.4 | UV-damage protection assays

Plates were seeded with HaCaT or HEK-293T cells, and they were incubated with a range of atoxic concentrations of NB or BE, as determined in 2.7.2.

Doses of UVA, UVB, or UVC that lowered the viability of HaCaT or HEK-293T cells to a 50% in the photodamage assay of 2.7.3. were chosen for each case, and then irradiated with the ad hoc systems. HaCaT cells were irradiated with UVA, UVB, and UVC, while HEK-293T only with UVC. Nonincubated cells were used as control. After 30 minutes (for UVC) or 24 h (for UVA and UVB), MTT assay was performed to determine the protective effect of the formulations on the cells.

3.3.5 | Cell capture assay

With the aim of study the ability of HaCaT cells to incorporate NB, cells were seeded for 24 h on coverslips placed on the bottom of 6-well multiplates and then incubated with FNB for 3 h at 37°C , before being intensively washed with PBS. RAW 264.7 were used as a positive phagocytosis control. Coverslips were observed with a Nikon Alphaphot-2 YS2 fluorescence microscope.

3.3.6 | Wound assay on cell culture

HaCaT cells were seeded for 24 h, initially at 4×10^4 cells per well, in a 12-well multiplate. Wounds on the near-confluent monolayers were performed by linear scratching with a plastic tip for 1-mL micropipette, based on a well-described method.²⁶ Wounded monolayers were then incubated with NB (at 2 mg/mL of BE for 0.5, or 3 h), BE (2 mg/mL, 0.5 h), or just with RPMI medium. After incubation time, formulations were removed and replaced by fresh medium, and then left growing for a total of 36 h after being wounded. Cells were fixed with cold methanol, stained with methylene blue, and observed with a trinocular magnifying glass equipped with an image capture system.

4 | RESULTS AND DISCUSSION

4.1 | BE and liposomal formulations

The BE contained 12 mg of polyphenols per gram. The total amount of anthocyanins (566 mg/100 g of BE) was into the expected range for berries.²⁷ Previous works have shown the direct relation between the phenolic content and antioxidant activity.¹²

Liposome preparation rendered NB of 113.7 ± 0.7 nm (zeta average by DLS), with 0.26 of polydispersity and -17.4 mV of

ζ -potential. Encapsulation efficiency was around 80% for all formulations. Similar values were recorded for NUNB, while for MNB, size was remarkably higher (608.2 ± 12.9 nm, 0.324 polydispersity). The ζ -potential of NB was similar to previous reports, according to which there was no aggregation or coalescence over more than 1 month.¹²

4.2 | Size and morphology by SEM

Scanning electronic microscopy showed small spherical vesicles for NB in both tested conditions (Figure 1). Previous works demonstrated that empty ultradeformable liposomes do not keep size and structure after vacuum dry without high presence of protectants.²¹ Thus, the absence of coalescence when the sample was dried without sucrose could show that the compounds present in the BE—specially sugars—could also act as structure protectants.

4.3 | Rheology and viscoelasticity

The rheological behavior showed a non-Newtonian flux, with pseudoplastic character²⁸ for both samples in both tested conditions, as shown in Figure 2. The consistency index was higher at 37°C than at 4°C, and higher for NB-C than for C. This behavior could be due to the presence of polyphenols from the extract acting as thickening agents in the gel.²⁹ A gel with those flux parameters is supposed to cause a good sensorial impression after application onto the skin.³⁰

The stress sweep step, as shown in Figure 3, clearly revealed the linear viscoelastic region, from which the τ of 1 Pa was chosen for the frequency sweep step. G' was always higher than G'' (Figure 4) revealing a solid elastic character independently of the NB presence or the temperature, which reflects that the addition of NB did not affect the good elastic properties of the gel in the studied frequency range.³¹

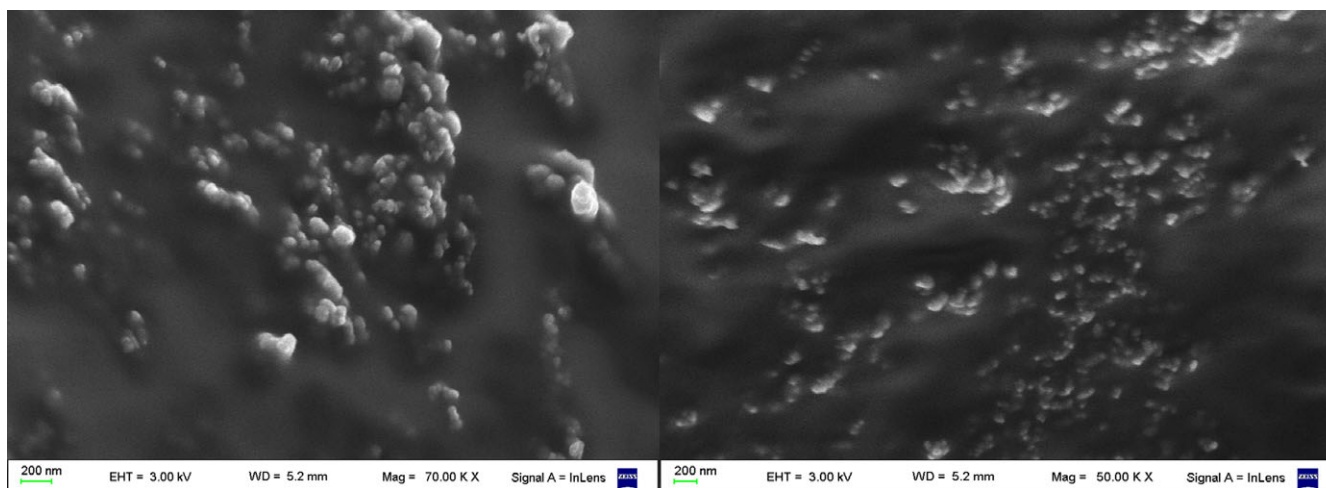


FIGURE 1 SEM images of vacuum-dried NB without sucrose (left) and in 20% sucrose (right)

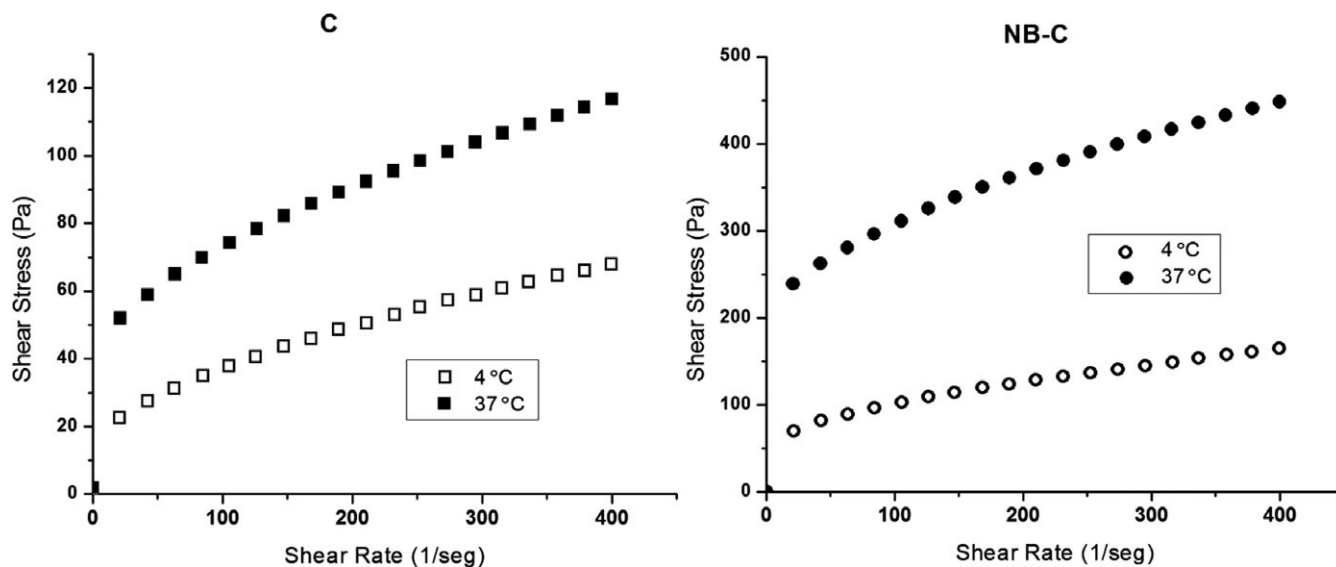


FIGURE 2 Rheograms for the Carbopol gel (left) and NB-C (right) at 4 and 37°C

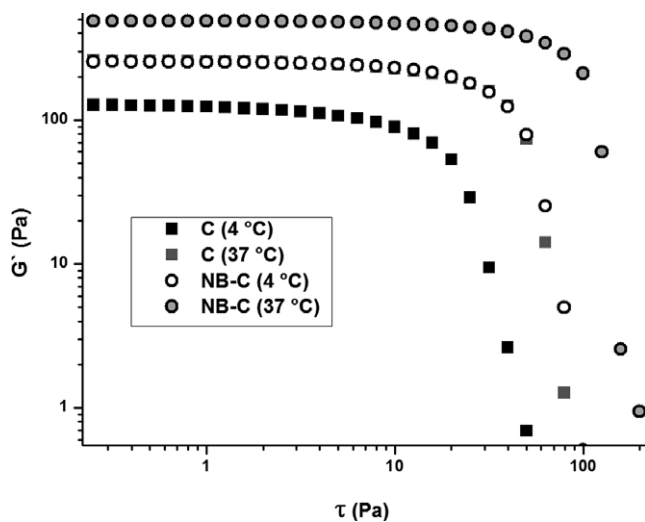
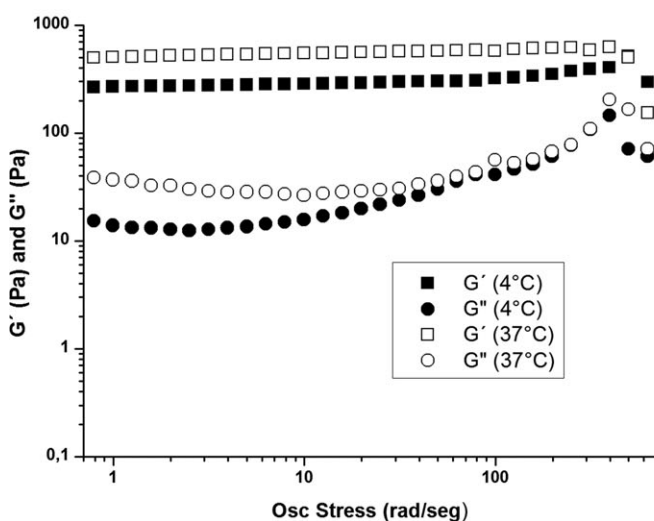


FIGURE 3 Stress sweep step for both formulations at 4 and 37°C. Frequency was fixed at 1 Hz. At a shear stress of 1 Pa, the samples of all the formulations were into their linear viscoelastic region

4.4 | In vivo nanotoxicity in zebrafish model

Swimming activities at 24, 48, and 72 hours postincubation (hpi) are shown in Figure 5. Values under the dotted line at 0.5 indicate treatments that lowered the normal activity in more than a 50%. At 24 hpi, this effect could be seen at 1.3 mg/mL only for BE. At 48 hpi, the effect of BE is similar, while NB also causes toxicity from that same low concentration. This could indicate that the free extract is toxic in the short term, while the NB toxicity appears in the midterm because of a progressive release of the liposome content. At 72 hpi, the empty liposomal matrix produces the toxic effect at the lipid concentration corresponding to 2.60 mg/mL of BE-loaded NB, while the NB are more toxic than the BE for all concentrations at this long term. This last result is in concordance with



LD₅₀ values (Table 1), which could indicate that at 72 hpi, the toxicity could be addressed to both the extract and the lipid matrix.

4.5 | Skin penetration of formulations

NB-C and NB were more effective than all the other formulations to carry the BE through all the SC, and to the viable epidermis, as shown in Figure 6A and B, respectively. As NUNB (with the same structure as NB) and MNB (with the same lipid composition as NB) delivered much less BE to the SC and epidermis than NB or NB-C did, it can be seen that the success of NB for skin penetration is remarkably due to the concurrence of both their composition and unilamellar structure.

The detailed SC-penetration profiles of fluorescent formulations (Figure 7) revealed higher values for FNB in comparison with FNUNB at every SC layer. Analysis of the penetration of FNB by optical sectioning CLSM (Figure 8) revealed a concordance between depths reached by both fluorescent markers, which could indicate that FNB did not lose integrity along the penetration path. On the other hand, transversal cryosections of skin samples showed the presence of the fluorescent labels of the lipid matrix (Rhodamine-PE) and inner aqueous content (FITC) along the whole thickness of the SC (Figure 9).

4.6 | UV-damage protection

Cytotoxicity determinations did not show diminution of viability when NB concentration was under 2.48 mg/mL of BE for HaCaT cells and 1.24 mg/mL for HEK-293T cells. Significant diminution of viability was found for both cell lines at 4.98 mg/mL (Figure 10). The results in HaCaT cells were in accordance with previous findings.¹² A concentration range, mainly nontoxic, was chosen in consequence for the experiments that followed.

Cells were then exposed to irradiation doses that lowered the viability for MTT assay to a 50% with respect to nonirradiated

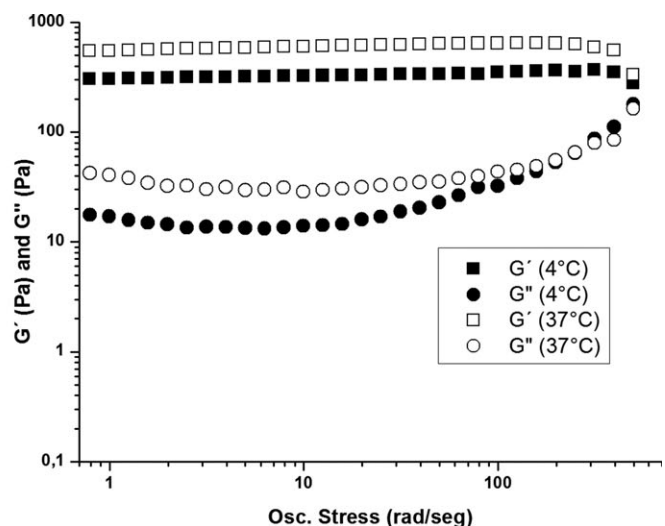


FIGURE 4 Frequency sweep step at $\tau = 1$ Pa showing the viscoelastic curves of G' and G'' at 4 and 37°C for C (left) and NB-C (right)

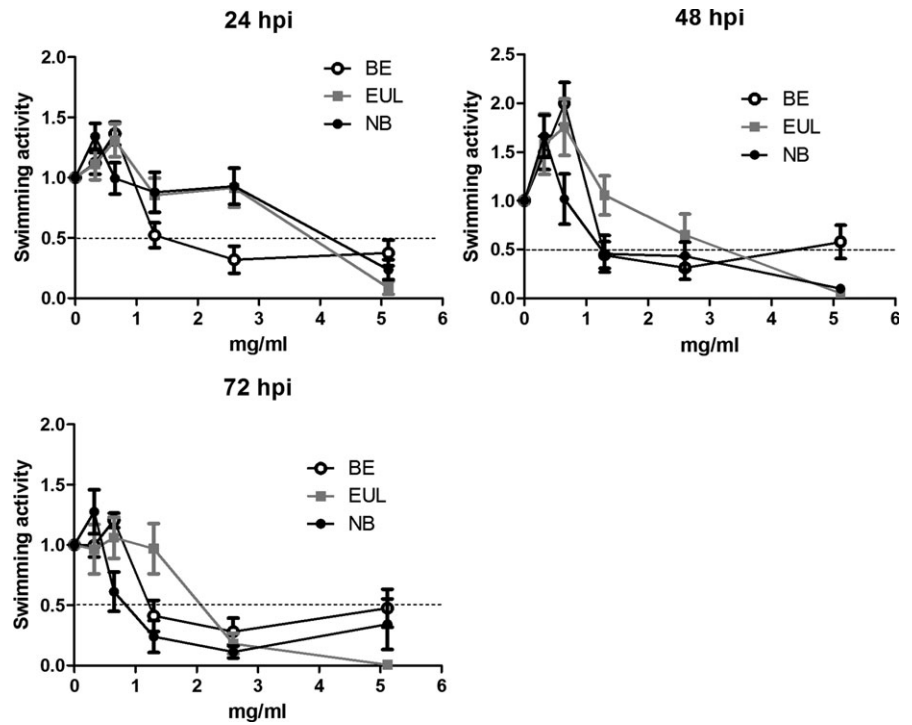


FIGURE 5 Swimming activity of zebrafish at 24, 48, and 72 hpi. Concentrations are expressed in mg of BE per mL. For EUL, values correspond to the BE content in NB at the same lipid concentration

TABLE 1 In vivo toxicity of the treatments. First three columns show the minimal concentrations that lower the swimming activity below 0.5 at 24, 48, and 72 hpi, respectively. The fourth column shows the LD₅₀ values after the last day of treatment

	24 hpi	48 hpi	72 hpi	LD ₅₀
BE (mg/mL)	1.4	1.3	1.3	2.8 ± 0.32
EUL (mg/mL)	3.9	3.3	2.1	0.55 ± 0.19
NB (mg/mL)	4.3	1.3	0.9	0.33 ± 0.36

controls, for each type of radiation: 14.4 J/cm² for UVA, 5.6 J/cm² for UVB, and 0.5 J/cm² for UVC in both HaCaT and HEK-293T cells.

Figure 11 shows the effects of incubation with NB or BE on reducing that photodamage. For UVA exposure, yet the lower tested concentration was effective to reduce the photodamage, with higher viability for NB-incubated than for free BE-incubated cells. As the BE concentration increases, the toxicity effect competes with the

FIGURE 6 Penetration of formulations into the SC (left) and the viable epidermis (right)

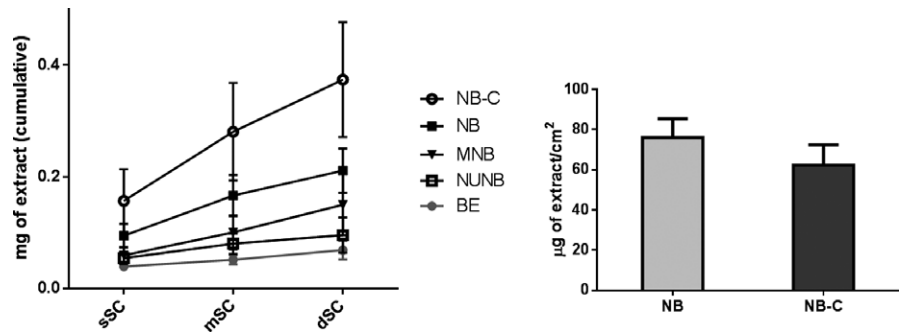
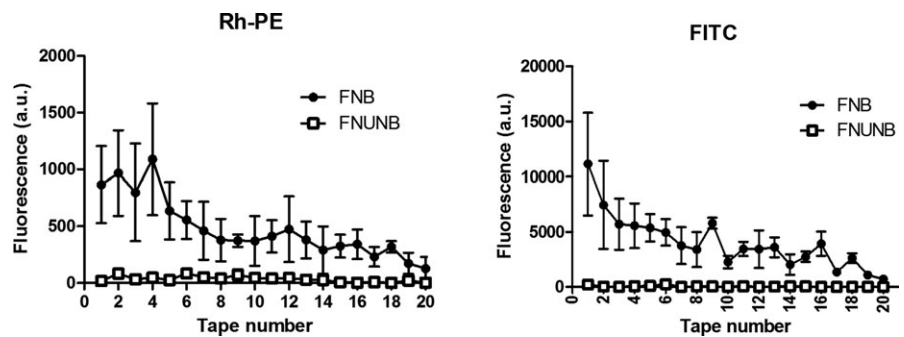


FIGURE 7 Skin penetration of Rh-PE (left) and FITC (right) in FNB along 20 strips of SC. The difference was highly significant ($P < .0001$) for both cases



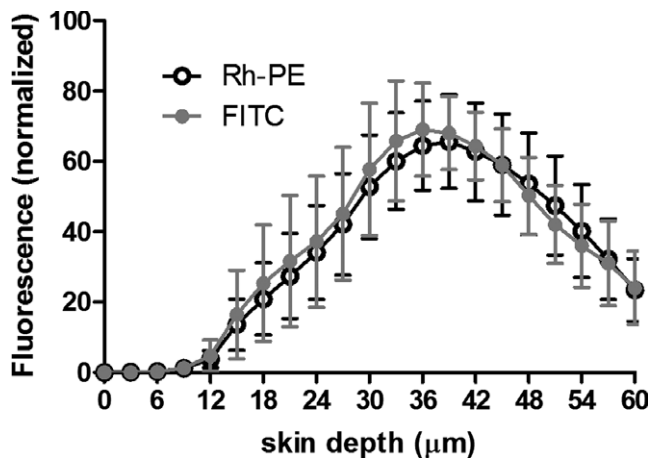


FIGURE 8 Fluorescence of FNB by optical sectioning in CLSM. Values were normalized to be comparable to each other

photoprotection and the viability decreases, although for NB there is still a protective action at high concentrations.

For UVB, photoprotection was achieved only when incubating with NB in the atoxic range, while BE incubation did not show differences from the irradiated control.

For UVC, a highly protective effect was determined for both formulations in all the studied range. It is interesting to note that viability was significantly higher than the irradiated control, even at concentrations in which toxicity competes with the protective effect of the formulations.

Finally, protection against UVC damage was also tested in HEK-293T, a kidney-derived cell line, with the aim of studying the protection of a cell type normally not exposed to UV radiation. A total revert of the damage effect was seen for the last nontoxic concentration (0.77 mg/mL), while for higher concentrations, the protective effect is also seen, but viabilities start to be lowered by the cytotoxic effect of the formulations.

Remarkably, the BE—delivered both as free formulation and as NB-incorporated—was effective to reduce the damage caused by

exposure to all types of UV radiation. This effect was observed when cultures were irradiated in the presence of concentrations of BE in the same range of those that showed antioxidant activity. Nevertheless, further studies could be conducted to elucidate in detail the mechanisms involved in skin photoprotection.

While the most energetic radiation, UVC, is filtered at the ozone layer, UVB is responsible of erythema, sunburns, and carcinogenic effects.³² UVA is, in principle, the less dangerous radiation but, on the other hand, the most penetrating, reaching the dermis activating matrix metalloproteinases (MMPs) which degrade collagen and other important molecules thus being, in long term, responsible for the aging of the skin.³³ UVA radiation has also been pointed as a possible long-term effector for carcinogenicity.³⁴ Despite the theoretically low penetrance of UVB, mainly limited to the viable epidermis, its role in damage at the dermis level by also activating MMPs has been proved³⁵ and thus pointed as a key factor in photoaging.³⁶ Thus, an effective delivery system for BE, as the NB proves to be, could protect the skin at more than one level, remarkably taking into account that the success of antioxidants to prevent the rapid events of damage induced by UV radiation depends on the disponibility of the drug at the site of action during the oxidative stress.³⁷

4.7 | Liposome capture

Cell uptake of FNB is shown in Figure 12. A macrophage-derived line such as RAW 264.7 rapidly phagocytosed and processed ultradeformable liposomes of around 100 nm, while in HaCaT, a similar fluorescence intensity was registered after longer incubation times. For both cell lines, the inner content of the liposomes was finally delivered to cytosol.

4.8 | Wound repair assay

The effects of the formulations on HaCaT cells are shown in Figure 13. After 30-min incubation, cell grow was notably higher when incubated with BE (b) in comparison with control (a), while NB

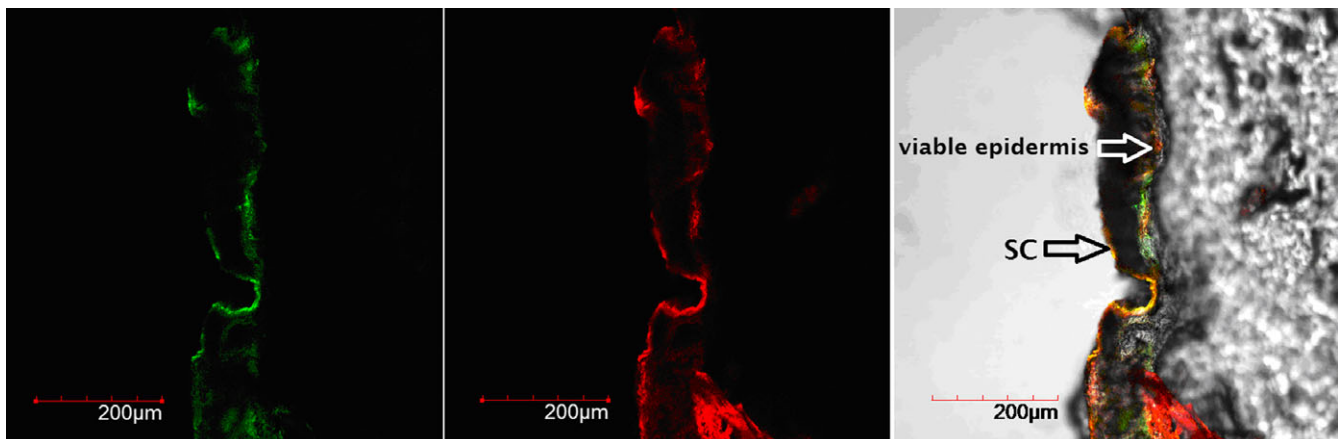


FIGURE 9 Transversal section of a skin sample after incubation with FNB. Fluorescence of FITC (left) and rhodamine (middle) and overlay of both marks with optical image (right)

incubation did not show differences from control. The repairing action could be due to the polyphenols of the BE, as it was suggested before,³⁸ even after a short time of exposure to the

formulation. At that short incubation time, NB are not effectively captured (in 3.7. was stated that it takes longer times for FNB capture by HaCaT cells). When incubation of NB was longer (3 h), a slightly higher grow was induced (d). A possible explanation is that the liposomes are captured but still not totally processed by the cells to liberate their content. These results could also be related to those from 3.6 where a proliferative effect could be seen in comparison with nonirradiated controls.

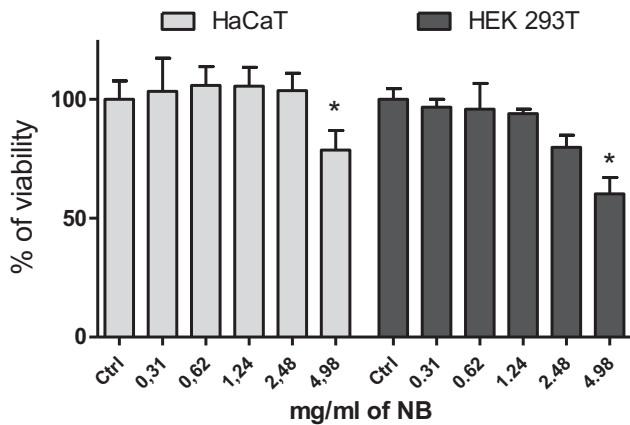


FIGURE 10 Cytotoxicity of NB in HaCaT (left, light gray) and HEK-293T (right, dark gray). * $P < 0.05$

5 | CONCLUSIONS

Nanoberries could be an effective system for the topical delivery of antioxidants, with the aim of protecting the skin from environmental photodamage. Their inclusion into a gel not only did not affect its parameters but also skin penetration was improved. NB can be actively captured by cells, and the compounds they transport have interesting properties for the skin health in terms of protection from different UV-radiation types and wound repair. A gel including NB

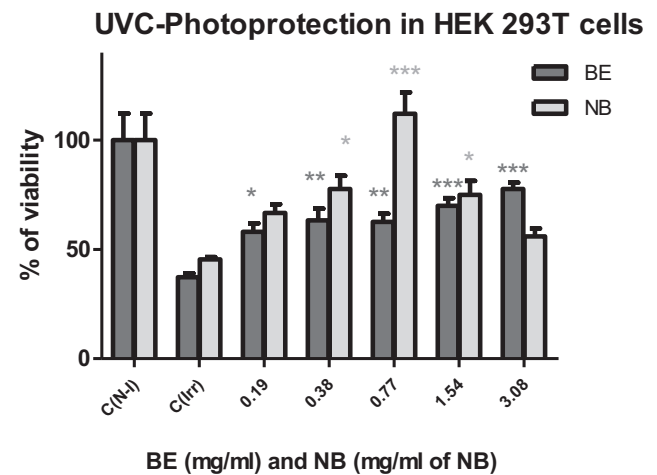
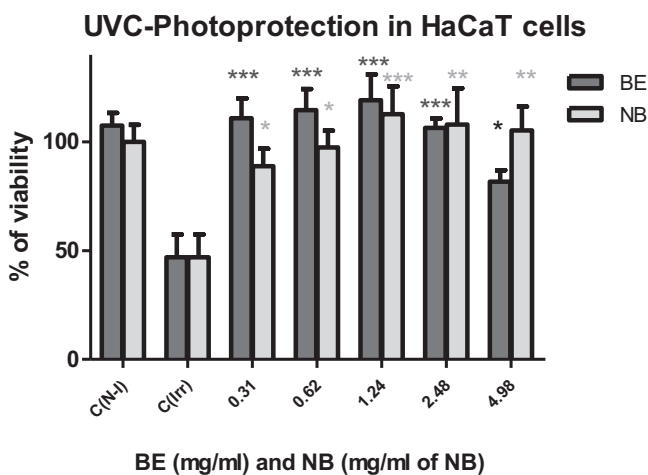
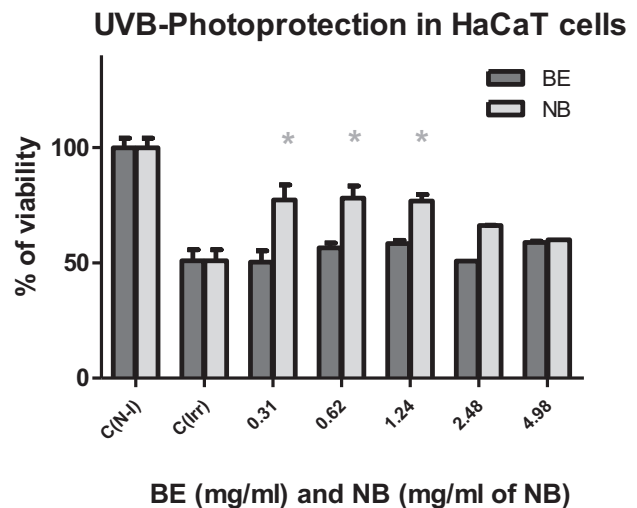
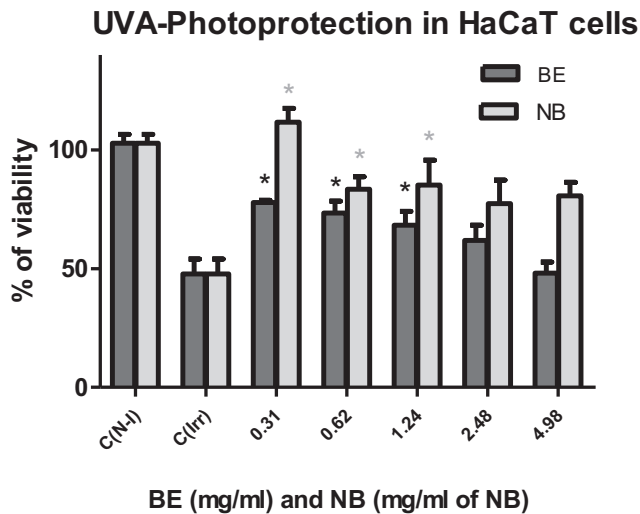


FIGURE 11 Photoprotection assays showing viability after irradiation with UVA (14.4 J/cm^2) on HaCaT cells (up, left); UVB (5.6 J/cm^2) on HaCaT cells (up, right); UVC (0.5 J/cm^2) on HaCaT cells (down, left) and UVC (0.5 J/cm^2) on HEK-293T cells. "C(N-I)" are the nonirradiated controls, while "C(Irr)" are the irradiated controls that were not protected with any formulation. * $P < 0.05$, ** $P < 0.0065$, *** $P < 0.0001$

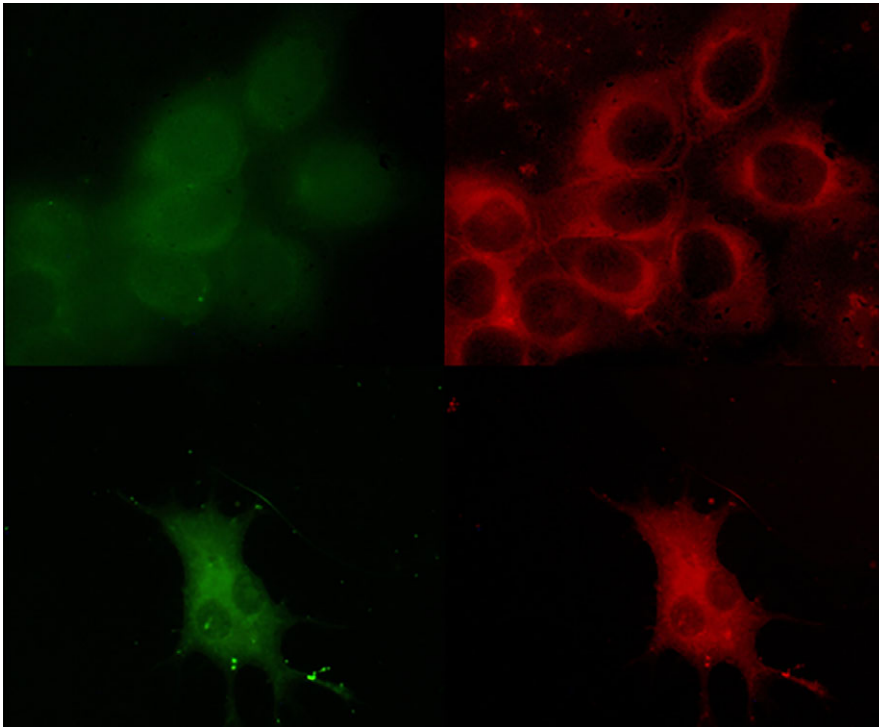


FIGURE 12 Cell uptake of FNB in HaCaT cells (up) and RAW 264.7 (down). FITC fluorescence is shown at left and Rh-PE at right

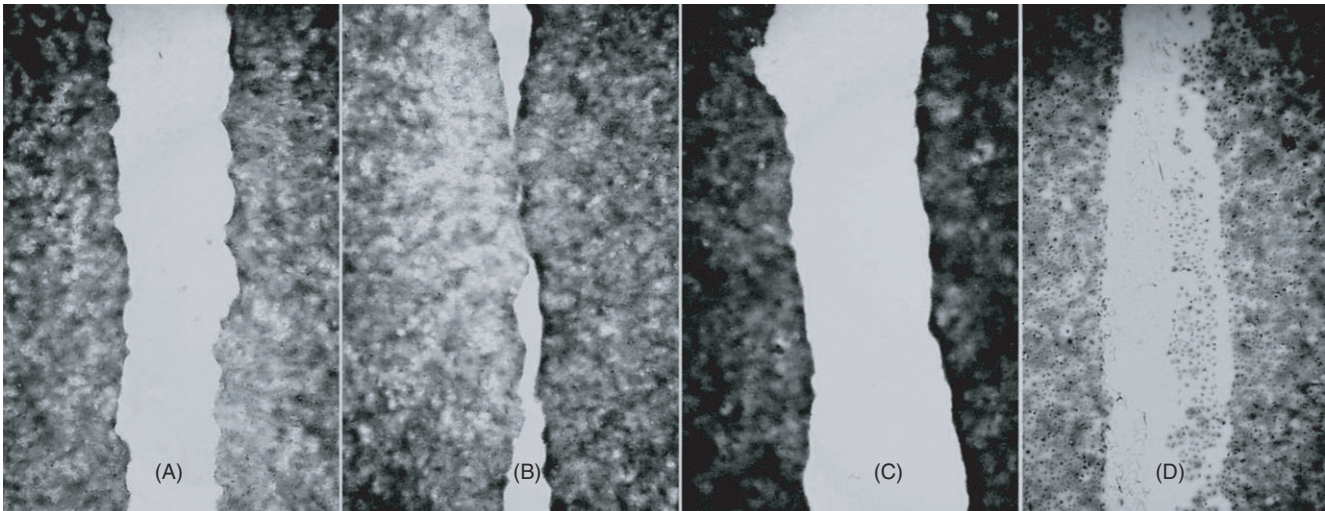


FIGURE 13 Wounds in HaCaT cultures after 36 h. A, Control without treatment; B, 30-min BE; C, 30-min NB; D, 3-h NB

for topical use could be a product of interest because of its cosmetic potential.

ACKNOWLEDGMENTS

Montanari, Prieto, Alonso, Rivarola and Milla are researchers from CONICET (National Council of Science and Technology Research in Argentina). We thank Dr. Humberto Jimenez for skin explants obtention, Dr. E. Salvatierra from Fundación Instituto Leloir for the supply of HaCaT cells, Rodrigo Palacios (Chemistry Department, UNRC) for his help on wavelength determinations, Dr. Rebeca Oliveira de Souza (USP, Brazil) for her invaluable help on development

of irradiation experiments, and The Berry Store for providing the blueberries.

ORCID

Jorge Montanari  <http://orcid.org/0000-0002-9177-0240>

REFERENCES

1. Harborne JB. 1 - General procedures and measurement of total phenolics. In: Harborne JB, ed. *Methods in Plant Biochemistry: 1. Plant Phenolics*. New York and London: Academic Press; 1989.

2. Kähkönen MP, Heinämäki J, Ollilainen V, et al. Berry anthocyanins: isolation, identification and antioxidant activities. *J Sci Food Agric*. 2003;83:1403-1411.
3. Seeram NP. Berry fruits: compositional elements, biochemical activities, and the impact of their intake on human health, performance, and disease. *J Agric Food Chem*. 2008;56:627-629.
4. Hirose M, Takesada Y, Tanaka H, et al. Carcinogenicity of antioxidants BHA, caffeic acid, sesamol, 4-methoxyphenol and catechol at low doses, either alone or in combination, and modulation of their effects in a rat medium-term multi-organ carcinogenesis model. *Carcinogenesis*. 1998;19:207-212.
5. Manach C, Williamson G, Morand C, et al. Bioavailability and bioefficacy of polyphenols in humans. I. Review of 97 bioavailability studies. *Am J Clin Nutr*. 2005;81:230S-242S.
6. Lipinski CA, Lombardo F, Dominy BW, et al. Experimental and computational approaches to estimate solubility and permeability in drug discovery and development settings. *Adv Drug Deliv Rev*. 2012;64:4-17.
7. Angosto MC, Gómez JAA. Metaloproteinasas, matriz extracelular y cáncer. *An R Acad Nac Farmac*, 2010;76:59-84.
8. Bae SH, Park JJ, Song EJ, et al. The comparison of the melanin content and UV exposure affecting aging process: seven countries in Asia. *J Cosmet Dermatol*. 2016;15:335-342.
9. Linos E, Li W, Han J, et al. Lifetime UV exposure and Lentigo Maligna Melanoma. *Br J Dermatol*. 2017;176:1666-1668.
10. Antonov D, Hollunder M, Schliemann S, et al. Ultraviolet exposure and protection behavior in the general population: a structured interview survey. *Dermatology*. 2015;232:11-16.
11. Alves Gd AD, de Souza RO, Rogez H, et al. Cecropia obtusa, an Amazonian ethanolic extract, exhibits photochemoprotective effect in vitro and balances the redox cellular state in response to UV radiation. *Ind Crops Prod*. 2016;94:893-902.
12. Montanari J, Vera M, Mensi E, et al. Nanoberrries for topical delivery of antioxidants. *J Cosmet Sci*. 2012;64:469-481.
13. Cevc G, Blume G. Lipid vesicles penetrate into intact skin owing to the transdermal osmotic gradients and hydration force. *Biochimica Biophys Acta* 1992;1104:226-232.
14. Montanari J, Maidana C, Esteva MI, et al. Sunlight triggered photo-dynamic ultradeformable liposomes against *Leishmania braziliensis* are also leishmanicidal in the dark. *J Controlled Release*. 2010;147:368-376.
15. Hernández I, Martinetti Montanari J, Escobar Rivero P. In vitro activity against *Leishmania* and human skin permeation of miltefosine ultradeformable liposomes. *Rev Cubana Med Trop*. 2014;66:370-385.
16. Li D, Wu Z, Martini N, et al. Advanced carrier systems in cosmetics and cosmeceuticals: a review. *J Cosmet Sci*. 2011;62:549-563.
17. Chandler S, Dodds J. The effect of phosphate, nitrogen and sucrose on the production of phenolics and solasodine in callus cultures of *Solanum laciniatum*. *Plant Cell Rep*. 1983;2:205-208.
18. Nicoue EE, Savard S, Belkacemi K. Anthocyanins in wild blueberries of Quebec: extraction and identification. *J Agric Food Chem*. 2007;55:5626-5635.
19. Fry DW, White JC, Goldman ID. Rapid separation of low molecular weight solutes from liposomes without dilution. *Anal Biochem*. 1978;90:809-815.
20. Al-Suwayeh SA, Taha EI, Al-Qahtani FM, et al. Evaluation of skin permeation and analgesic activity effects of carbopol lornoxicam topical gels containing penetration enhancer. *Sci World J*. 2014;2014:127495, <http://org.doi/10.1155/2014/127495>.
21. Montanari J, Roncaglia D, Lado L, et al. Avoiding failed reconstitution of ultradeformable liposomes upon dehydration. *Int J Pharm*. 2009;372:184-190.
22. Prieto MJ, del Rio Zabala NE, Marotta CH, et al. G4. 5 pamam dendrimer-risperidone: biodistribution and behavioral changes in in vivo model. *J Nanomedicine Biotherapeutic Discov*. 2013;4:121. <http://org.doi/10.4172/2155-983X.1000121>.
23. Igartúa DE, Calienni MN, Feas DA, et al. Development of nutraceutical emulsions as risperidone delivery systems: characterization and toxicological studies. *J Pharm Sci*. 2015;104:4142-4152.
24. Schaefer U, Loth H. An ex-vivo model for the study of drug penetration into human skin. *Pharm Res*. 1996;13:b24.
25. Mosmann T. Rapid colorimetric assay for cellular growth and survival: application to proliferation and cytotoxicity assays. *J Immunol Methods*. 1983;65:55-63.
26. Liang C-C, Park AY, Guan J-L. In vitro scratch assay: a convenient and inexpensive method for analysis of cell migration in vitro. *Nat Protoc*. 2007;2:329-333.
27. Böhm H. In Mazza G, Miniati E, eds. *Anthocyanins in Fruits, Vegetables and Grains*. 362 Seiten, zahlr. Abb. und Tab. Boca Raton, Ann Arbor, London, Tokyo: CRC Press; 1993. Preis: 144.—£. Food/Nahrung 1994;38:343-343.
28. Steffe JF. *Rheological Methods in Food Process Engineering*. East Lansing, MI, USA: Freeman press; 1996.
29. Daudt RM, Back PI, Cardozo NSM, et al. Pinhão starch and coat extract as new natural cosmetic ingredients: topical formulation stability and sensory analysis. *Carbohydr Polym*. 2015;134:573-580.
30. Guaratini T, Gianeti MD, Campos PM. Stability of cosmetic formulations containing esters of Vitamins E and A: chemical and physical aspects. *Int J Pharm*. 2006;327:12-16.
31. Baek G, Kim C. Rheological properties of Carbopol containing nanoparticles. *J Rheology (1978-Present)* 2011;55:313-330.
32. Saéz-de Ocariz M, Orozco-Covarrubias M. Protección solar en el paciente pediátrico. *Acta Pediátrica de México*. 2015;36:364-368.
33. Quan T, Qin Z, Xia W, et al. Matrix-degrading metalloproteinases in photoaging. *J Investig Dermatol Symp Proc*. 2009;14:20-24.
34. He Y, Pi J, Huang J, et al. Chronic UVA irradiation of human HaCaT keratinocytes induces malignant transformation associated with acquired apoptotic resistance. *Oncogene*. 2006;25:3680-3688.
35. Sárdy M. Role of matrix metalloproteinases in skin ageing. *Connect Tissue Res*. 2009;50:132-138.
36. Fisher GJ, Kang S, Varani J, et al. Mechanisms of photoaging and chronological skin aging. *Arch Dermatol*. 2002;138:1462-1470.
37. Dreher F, Denig N, Gabard B, et al. Effect of topical antioxidants on UV-induced erythema formation when administered after exposure. *Dermatology*. 1999;198:52-55.
38. Yan H, Peng K, Wang Q, et al. Effect of pomegranate peel polyphenol gel on cutaneous wound healing in alloxan-induced diabetic rats. *Chin Med J*. 2012;126:1700-1706.

How to cite this article: Bucci P, Prieto MJ, Milla L, et al. Skin penetration and UV-damage prevention by nanoberrries. *J Cosmet Dermatol*. 2017;00:1-11. <https://doi.org/10.1111/jocd.12436>